

Theoretical Study of Gallium Nitride Molecules, GaN₂ and GaN₄.

Demeter Tzeli,* Giannoula Theodorakopoulos, and Ioannis D. Petsalakis

Theoretical and Physical Chemistry Institute, National Hellenic Research Foundation, 48 Vassileos Constantinou Avenue, Athens GR-116 35, Greece

Received: March 5, 2008; Revised Manuscript Received: May 29, 2008

The electronic and geometric structures of gallium dinitride GaN₂, and gallium tetranitride molecules, GaN₄, were systematically studied by employing density functional theory and perturbation theory (MP2, MP4) in conjunction with the aug-cc-pVTZ basis set. In addition, for the ground-state of GaN₄(²B₁) a density functional theory study was carried out combining different functionals with different basis sets. A total of 7 minima have been identified for GaN₂, while 37 structures were identified for GaN₄ corresponding to minima, transition states, and saddle points. We report geometries and dissociation energies for all the above structures as well as potential energy profiles, potential energy surfaces and bonding mechanisms for some low-lying electronic states of GaN₄. The dissociation energy of the ground-state GaN₂($\tilde{X}^2\Pi$) is 1.1 kcal/mol with respect to Ga(²P) + N₂($X^1\Sigma_g^+$). The ground-state and the first two excited minima of GaN₄ are of ²B₁(C_{2v}), ²A₁(C_{2v}, five member ring), and ⁴Σ_g⁻(D_{∞h}) symmetry, respectively. The dissociation energy (D_e) of the ground-state of GaN₄, \tilde{X}^2B_1 , with respect to Ga(²P) + 2 N₂($X^1\Sigma_g^+$), is 2.4 kcal/mol, whereas the D_e of ⁴Σ_g⁻ with respect to Ga(⁴P) + 2 N₂($X^1\Sigma_g^+$) is 17.6 kcal/mol.

I. Introduction

Gallium nitrides are semiconducting materials with promising technological applications in microelectronics, nanomaterials, and optics.^{1–3} Consequently a significant number of experimental and theoretical studies of the electronic, structural, and optical properties of the solid phase material have been reported in the literature.⁴ Information on the geometry and electronic structure of small GaN clusters is essential for applications in microelectronics, yet work on such clusters either experimental or theoretical is less common, with publications of the latter kind being on the rise lately.

Several theoretical studies on Ga_xN_y species have been reported, for example on symmetric molecules, Ga_nN_n (n = 1–6^{5–8}), but not many for the systems of interest here. For GaN₂ three previous studies exist: Kandalam et al.⁹ employing density functional theory (DFT) calculations found 3 isomers. Zhou et al.¹⁰ presented the spectra of laser-ablated Ga atoms codeposited with pure nitrogen and some DFT calculations where two states of GaN₂ were determined but not the ground state. In 2004, Wang et al.¹¹ using DFT, Møller–Plesset Perturbation theory (MP2) and Coupled-Clusters methods (CCD) calculated four isomers of the GaN₂ molecule. For the case of GaN₄, there is only one study, where Song et al.¹² using the full potential linear muffin tin orbital method calculated three isomers. Thus, a comprehensive and systematic theoretical study of the possible stable structures of GaN₂ and GaN₄ were not pursued in these previous reports.

In the present work, which is a continuation of our previous work on the corresponding cations GaN₂⁺ and GaN₄⁺,¹³ gallium dinitride and tetranitride molecules, GaN₂ and GaN₄, were systematically studied using both DFT and MP (MP2, MP4) techniques. In total, 7 minima for GaN₂ and 37 structures for GaN₄ were determined corresponding to minima, transition states, and saddle points. Total energies (E), binding energies (D_e), and geometries (r_e, angles) are reported for all 7 structures

of GaN₂ and for 17 of GaN₄, while the corresponding data for the remaining 20 isomers (minima, transition states, and saddle points) calculated for GaN₄ are provided as Supporting Information. Moreover, vibrational frequencies, potential energy profiles (PEP), and two-dimensional sections of potential energy surfaces (PES) of some low-energy structures of GaN₂ and GaN₄ are plotted. Finally, the bonding process for selected structures is discussed.

In Section II, we describe the computational procedure followed, in Section III we discuss our results on the GaN₂ molecule, in Section IV our results on GaN₄, and, finally, in Section V we present some conclusions and comments.

II. Computational Procedure

For the GaN₂ molecule, the lowest lying, spin doublet and quartet, linear and bent (NNGa, NGaN) structures were calculated giving seven distinct species. For GaN₄, a preliminary sampling of the configuration space and bonding networks was performed using the electronic structures of the combining fragments N₄ + Ga, N₃ + Ga + N, N₂ + GaN₂, GaN₃ + N, and GaN₂ + 2N. About 80 structures were examined for stability resulting in 37 spin doublet and quartet geometry optimized electronic structures of GaN₄ at the B3LYP/LANL2DZ level of theory. B3LYP is a DFT functional using Becke's three parameter gradient corrected functional¹⁴ with the gradient corrected correlation of Lee, Yang, and Parr.¹⁵ The Hay-Wadt LANL2DZ ECP¹⁶ basis set consists of a pseudopotential for the core electrons (up to 3d electrons) of Ga and a double-ζ quality basis set, for the three outer electrons of Ga, (4s²4p¹), and the seven electrons of N, i.e., (3s3p) → [2s2p]_{Ga} and (10s5p) → [3s2p]_N. Moreover, additional calculations have been carried out for the ground-state of GaN₄ (²B₁), which is a van der Waals isomer, in order to test the limits of reliability of the different theoretical procedures. The DFT method was used with various combinations involving 4 functionals [B3LYP,^{14,15} B3PW91,¹⁷ PBEPBE,¹⁸ and LSDA¹⁹] and 10 basis sets [LANL2DZ,¹⁶ DGDZVP,²⁰ cc-pVDZ,²¹ SDD,²² 6-311,²³

* Corresponding author. E-mail: dtzeli@eie.gr. Fax: +30-210-7273-794.

TABLE 1: Absolute Energies E_e (h), Geometries $r_{\text{Ga-N}}$, $r_{\text{N-N}}$ (Å), φ (degrees), Dissociation Energies with Respect of Ga + 2N, D_{e1} (kcal/mol) and Ga + N₂, D_{e2} (kcal/mol) and Relative Energy ΔE (kcal/mol) of the GaN₂ Molecule

method	$-E$	$r_{\text{Ga-N}}$	$r_{\text{N-N}}$	φ	D_{e1} (BSSE) ^a	D_{e2} (BSSE) ^b	ΔE
² Ga-N-N(C _{∞v})				$\tilde{X}^2\Pi$			
B3LYP/LANL2DZ	111.510721	2.048	1.176	180.0	193.0(191.4)	11.68(8.04)	0.0
B3LYP/DGDZVP	2033.973475	2.447	1.121	180.0	220.7(219.9)	3.06(1.13)	0.0
B3LYP/6-311G+(2df)	2034.389912	2.742	1.097	180.0	230.4(229.4)	1.30(0.86)	0.0
MP2/6-311G+(2df)	2032.566167	3.321	1.113	180.0	231.2(227.7)	1.31(0.78)	0.0
MP2/cc-pVTZ	2032.724976	3.222	1.113	180.0	230.4(227.8)	1.61(0.91)	0.0
MP2/aug-cc-pVTZ	2032.735099	3.191	1.114	180.0	232.7(229.6)	2.10(1.03)	0.0
MP2 _{BSSSE} /aug-cc-pVTZ ^c	2032.730154	3.301	1.115	180.0	(229.6)		0.0
MP2 _{BSSSE} /aug-cc-pVTZ ^d	2032.733445	3.306	1.114	180.0		(1.06)	0.0
MP4/aug-cc-pVTZ ^e	2032.776804				225.0(222.3)	2.01(0.99)	0.0
² N-Ga-N(C _{2v})				I^2B_2			
MP2/aug-cc-pVTZ	2032.733356	3.554	1.115	18.1	231.6(228.7)	1.00(0.13)	1.09
MP2 _{BSSSE} /aug-cc-pVTZ ^c	2032.728827	3.845	1.116	16.7	(228.8)		0.83
MP2 _{BSSSE} /aug-cc-pVTZ ^d	2032.732149	3.879	1.115	16.5		(0.24)	0.81
⁴ Ga-N-N(C _{∞v})				$\tilde{a}^4\Sigma^-$			
MP2/aug-cc-pVTZ	2032.619328	1.964	1.088	180.0	250.0(243.0)	19.4(14.5)	72.6
MP2 _{BSSSE} /aug-cc-pVTZ ^c	2032.608174	2.000	1.088	180.0	(243.0)		76.5
MP2 _{BSSSE} /aug-cc-pVTZ ^d	2032.611433	2.002	1.087	180.0		(14.5)	76.6
⁴ N-Ga-N(C _{2v})				I^4A_2			
MP2/aug-cc-pVTZ	2032.604600	2.216	1.143	29.9	240.8(234.6)	10.2(5.81)	81.9
MP2 _{BSSSE} /aug-cc-pVTZ ^c	2032.594729	2.243	1.147	29.6	(234.6)		85.0
MP2 _{BSSSE} /aug-cc-pVTZ ^d	2032.597626	2.242	1.147	29.6		(5.81)	85.2
⁴ N-Ga-N(C _{2v})				I^4B_1			
MP2/aug-cc-pVTZ	2032.578491	1.932	1.254	37.9	224.4(216.3)	-6.20(-13.0)	98.3
MP2 _{BSSSE} /aug-cc-pVTZ ^c	2032.565594	1.948	1.257	37.6	(216.3)		103.3
MP2 _{BSSSE} /aug-cc-pVTZ ^d	2032.567832	1.948	1.257	37.6		(-12.9)	103.9
² N-Ga-N(D _{∞h})				$I^2\Pi_g$			
MP2/aug-cc-pVTZ	2032.486649	1.759	3.517	180.0	76.8(67.9)		155.9
MP2 _{BSSSE} /aug-cc-pVTZ ^c	2032.472567	1.767	3.534	180.0	(68.0)		161.6
⁴ N-Ga-N(D _{∞h})				$I^4\Pi_u$			
MP2/aug-cc-pVTZ	2032.470580	1.789	3.579	180.0	156.7(149.7)		166.0
MP2 _{BSSSE} /aug-cc-pVTZ ^c	2032.459488	1.796	3.592	180.0	(149.7)		169.8

^a D_e values of doublet and quartet states calculated with respect to the Ga(²P) and Ga(⁴P) + 2N(⁴S), respectively. ^b D_e values of doublet and quartet states calculated with respect to the Ga(²P) and Ga(⁴P) + N₂($X^1\Sigma_g^+$), respectively. ^c MP2 optimized geometry for BSSE correction with respect to Ga + 2N. ^d MP2 optimized geometry for BSSE correction with respect to Ga + N₂. ^e MP4/aug-cc-pVTZ//MP2/aug-cc-pVTZ.

6-311+²³ 6-311G(2df),²³ 6-311+G(2df),²³ 6-311+G(3df),²³ and aug-cc-pVTZ²¹]. Additionally, MP2 and MP4 calculations were carried out using the 6-311+G(2df),²³ cc-pVTZ,²¹ and aug-cc-pVTZ²¹ basis sets.

Subsequently, all 7 isomers of GaN₂ and the 17 lowest structures of GaN₄ were fully optimized at the unrestricted MP2/aug-cc-pVTZ level of theory, using second order perturbation theory and the augmented correlation-consistent basis of Dunning,²¹ aug-cc-pVTZ (referred to as atz), i.e., (21s14p10d2f) → [7s6p4d2f]_{Ga} and (11s6p3d2f) → [5s4p3d2f]_N, thus involving 151(GaN₂) and 243(GaN₄) contracted Gaussian functions. The 3d¹⁰4s²4p¹ electrons of the Ga atom and the 2s²2p³ electrons of the N atom have been correlated. As has been demonstrated previously for related systems (InN,²⁴ GaN,²⁵ Ga₂N²⁵), it is necessary to include the 3d¹⁰ electrons in the valence set, for the calculation of geometries and dissociation energies. In order to evaluate the importance of the contribution of the third and fourth order of perturbation theory to the calculated quantities, single point MP4(SDTQ)/atz//MP2/atz calculations were carried out for the lowest minima of both GaN₂ and GaN₄.

The harmonic frequencies of all 7 structures of GaN₂ and 37 of GaN₄ at DFT and MP2 level of theory were calculated so as to clarify whether they are minima or transition states and saddle points.

For all structures at all levels of theory, basis set superposition error (BSSE) corrections were made using the counterpoise procedure^{26,27} since such corrections are especially important for van der Waals systems,²⁸ which is the case for most of the

structures calculated here. Furthermore, MP2 geometry optimizations were carried out with respect to the BSSE-corrected energy²⁹ (MP2_{BSSSE} calculations) for all 7 structures of GaN₂.

Finally, it should be noted that there are no size nonextensivity problems in the plotting of the potential energy profiles of GaN₂ and GaN₄ with the relevant error being less than 7 μ h.

All the above DFT as well as MP calculations were performed using the Gaussian 03 program package.³⁰

III. GaN₂

We have calculated seven linear and bent structures which all were minimum energy structures $\tilde{X}^2\Pi$, I^2B_2 , $\tilde{a}^4\Sigma^-$, I^4A_2 , I^4B_1 , $I^2\Pi_g$, and $I^4\Pi_u$, listed here in increasing total energy order. Their total energies (E), geometries (r_e , angles), and dissociation energies with respect to the Ga(²P or ⁴P) + 2N(⁴S) (D_{e1}) and Ga(²P or ⁴P) + N₂($X^1\Sigma_g^+$) (D_{e2}), calculated with different computational procedures are presented in Table 1. The corresponding harmonic vibrational frequencies, IR intensities, and dipole moments at the MP2/atz level of theory are given in Table 2.

The three isomers of GaN₂ reported by Kandalam et al.⁹ using the DFT (GGA/DNP) method, correspond to our $\tilde{X}^2\Pi$, I^2B_2 , and $I^2\Pi_g$, cf. Table 1, but they reported the I^2B_2 isomer as the global minimum while their $r_{\text{Ga-N}}$ distances were significantly smaller than our MP2/atz results, by up to 1 Å. Moreover, they reported a dissociation energy of 6.00 kcal/mol with respect to Ga + N₂ compared to our 1.06 kcal/mol (MP2_{BSSSE}/atz, see

TABLE 2: GaN₂ Harmonic Frequencies ω_e (cm⁻¹), IR Intensities (km/mol), and Dipole Moments μ (Debye) at the MP2/aug-cc-pVTZ Level of Theory

	$\tilde{X}^2\Pi$		I^2B_2		$\tilde{a}^4\Sigma^-$		I^4A_2		I^4B_1		$I^2\Pi_g$		$I^4\Pi_u$	
	ω_e	IR	ω_e	IR	ω_e	IR	ω_e	IR	ω_e	IR	ω_e	IR	ω_e	IR
ω_1	42.2	0.12	31.8	0.17	281.6	54.9	372.3	87.9	202.0	0.51	269.0	765	114.1	49.6
ω_2	49.6	0.06	49.7	0.03	347.2	1.22	593.1	32.2	548.7	28.4	760.6	0	333.3	3115
ω_3	51.9	0.63	2173.7	1.3	347.2	1.22	2858.5	7759	3507.2	15868	990.8	380	535.9	1658
ω_4	2285.8	3.9			3201.7	1591					6764.2		693.6	0
μ	0.347		0.045		0.297		0.152		3.93		0		0	

below). As we will discuss below, the DFT method can give for some isomers of this molecule extremely small bond distances and large dissociation energies. In 2000, Zhou et al.¹⁰ determined two isomers of GaN₂ ($I^2\Pi_g$ and $I^4\Pi_u$), again using DFT calculations. These isomers are found in the present work to lie 162 and 170 kcal/mol, respectively, above our global minimum. In 2004, Wang et al.¹¹ calculated the $\tilde{X}^2\Pi$, I^2B_2 , $I^2\Pi_g$, and $I^4\Pi_u$ isomers of the GaN₂ molecule, using a relativistic effective core potential in conjunction with a double- ζ quality basis set for the 3d4s4p electrons of Ga and 2s2p electrons of N and keeping the 3d electrons inactive. All four structures were calculated by DFT-B3LYP while three of them using the MP2 and CCD methods. They found for the global minimum a shorter $r_{\text{Ga-N}}$ distance at their DFT level than to their MP2 and CCD. Furthermore, they found dissociation energies, with respect to Ga + N₂, 5.01, 2.31, and 1.84 kcal/mol at the B3LYP, MP2, and CCD, respectively. As shown in Table 1, our results are in agreement with those of Wang et al.,¹¹ regarding the energy ordering of the above four structures. However, our $r_{\text{Ga-N}}$ distance in $\tilde{X}^2\Pi$ is larger than their MP2 and CCD values by 0.4 Å while our best result for the dissociation energy is 1.06 kcal/mol at MP2_{BSSSE}/atz (see below). The differences are mainly due to the fact that our basis set is larger compared to theirs (augmented-triple- ζ vs double- ζ) and second, due to the BSSE optimization carried out in the present calculations (see also below).

The ground-state of the GaN₂ molecule, $\tilde{X}^2\Pi$, is linear, consisting of a ground-state nitrogen molecule, N₂($X^1\Sigma_g^+$), interacting via a der Waals (vdW) bond with the Ga(²P) atom. Both natural and Mulliken population analyses show practically no charge transfer. Our best geometry at MP2_{BSSSE}/atz (MP2/atz geometry which is optimized for the BSSE-corrected energy) level is $r_{\text{Ga-N}} = 3.306$ and $r_{\text{N-N}} = 1.114$ Å. The dissociation energy with respect to Ga + N₂, D_{e2} , is 1.06 kcal/mol at the MP2_{BSSSE}/atz level of theory. The MP4(SDTQ)/atz//MP2/atz dissociation energy is 1.0 kcal/mol, which is very close to the above MP2 value, suggesting that the MP2 method is sufficient. The spin contamination of the UMP2 calculation is very small with $\langle S^2 \rangle = 0.753$ instead of 0.75. Comparing the ground-state of GaN₂ ($\tilde{X}^2\Pi$) with that of the cation, GaN₂⁺($\tilde{X}^1\Sigma^+$), they are both linear vdW species of the same type, where the neutral has a longer $r_{\text{Ga-N}}$ bond by 0.5 Å and a smaller dissociation energy with respect to Ga + N₂ by 4 kcal/mol than the cation; see Table 1 and ref 13. Moreover, as in the case of the cation,¹³ we observe that augmentation of the basis set with diffuse functions (aug-) results in a shorter vdW bond length compared with the same quality nonaugmented basis set while geometry optimization with respect to the BSSE-corrected energy results in a longer vdW bond length.

As in Wang et al.,¹¹ here too the DFT (B3LYP) method is found to give shorter vdW distances than the MP2 method. For example, it gives a bond length shorter by 1.14 using the LANL2DZ basis set, by 0.74 using the DGDZVP, and by 0.45 Å using the 6-311G+(2df) than the value of the MP2_{BSSSE}/atz method. Moreover, the dissociation energy, D_{e2} , with respect

to Ga + N₂ is significantly overestimated for the LANL2DZ basis set ($D_{e2} = 8.0$ kcal/mol), while DGDZVP gives 1.13 kcal/mol very close to the 1.06 kcal/mol of the MP2_{BSSSE}/atz level of theory. However, the dissociation energy with respect to Ga + 2N is well described with the DFT methods (cf. Table 1).

The lowest energy bent structure of GaN₂, I^2B_2 is also a vdW structure with a Ga (²P) atom interacting with the triple bond of N₂($X^1\Sigma_g^+$) and forming a T-shaped molecule. This local minimum lies 0.8 kcal/mol above the global minimum at the MP2_{BSSSE}/atz level of theory. Both the $\tilde{X}^2\Pi$ and I^2B_2 minima are on the same potential surface. The dissociation energy of I^2B_2 (D_{e2}) with respect to Ga + N₂ is only 0.24 kcal/mol, the distance between Ga and the middle of the N≡N triple bond is rather large at 3.839 Å, and the angle φ_{NGaN} is 16.7° at the MP2_{BSSSE}/atz level of theory. Again the calculations show that there is practically no charge transfer between N≡N and Ga. Comparing the lowest bent structure of GaN₂(I^2B_2) with that of GaN₂⁺(I^1A_1), they are both T-shaped vdW species of the same type where the neutral has a longer $r_{\text{Ga-N}}$ bond by 0.4 Å and a smaller dissociation energy with respect to Ga+N₂ by 0.7 kcal/mol than the cation; see Table 1 and ref 13. The difference between these two lowest bent structures is that the I^2B_2 isomer of GaN₂ is a minimum while the I^1A_1 isomer of GaN₂⁺ is a transition structure.

The first excited-state of GaN₂ calculated here is the linear $\tilde{a}^4\Sigma^-$, correlating with 2 N(⁴S) + Ga(⁴P) and N₂($X^1\Sigma_g^+$) + Ga(⁴P). The Ga atom is connected to N₂ with a σ interaction (which is formed between the empty 4p_z orbital of Ga and the 2s² orbital of the adjacent N, where the first one gains about 0.2 e⁻) and two π interactions (between the 4p_x¹ orbital of Ga with the π_x ² orbital of N₂ and the 4p_y¹ orbital of Ga and the π_y ² orbital of N₂). The natural population analysis for this structure gives Ga the following: 4s^{0.99} 4p_z^{0.18} 4p_x^{0.84} 4p_y^{0.84}. The middle N atom gains about 0.2 e⁻. The dissociation energy with respect to Ga(⁴P) + N₂($X^1\Sigma_g^+$) is 14.5 kcal/mol at MP2_{BSSSE}/atz level of theory, and the vdW bond distance 2.002 Å at the same level. Thus the Ga-N bond length in the $\tilde{a}^4\Sigma^-$ state of GaN₂ is shorter than the corresponding bond length of the ground-state by 1.3 Å (cf. Table 1). The spin contamination of the UMP2 calculation is very small with $\langle S^2 \rangle = 3.80$ instead of 3.75.

The triangular I^4A_2 and I^4B_1 structures are minima, where Ga (⁴P) interacts with the ground-state N₂($X^1\Sigma_g^+$) and the excited-state N₂($a^3\Sigma_u^+$), respectively, as can be seen from the geometry and mainly by the population analysis and the orbitals. In the I^4A_2 minimum the bond lengths are $r_{\text{Ga-N}} = 2.242$ and $r_{\text{N-N}} = 1.147$ Å at the MP2_{BSSSE}/atz level of theory, see Table 1, and the dissociation energy with respect to Ga(⁴P) + N₂($X^1\Sigma_g^+$) is 5.81 kcal/mol. In the I^4B_1 minimum the bond lengths are $r_{\text{Ga-N}} = 1.948$ and $r_{\text{N-N}} = 1.257$ Å at the MP2_{BSSSE}/atz level of theory, see Table 1, which is close to the $r_{\text{N-N}}$ distance in free N₂($a^3\Sigma_u^+$); here it is calculated as 1.2886 Å at the MP2/atz level of theory (expt: 1.2866 Å³¹). The $a^3\Sigma_u^+$ state of N₂ is located 166.5 kcal/mol above the ground $X^1\Sigma_g^+$ state at the MP2/atz level of theory. The I^4B_1 state of GaN₂ is unbound with respect to Ga(⁴P) + N₂($X^1\Sigma_g^+$) (calculated D_{e2}

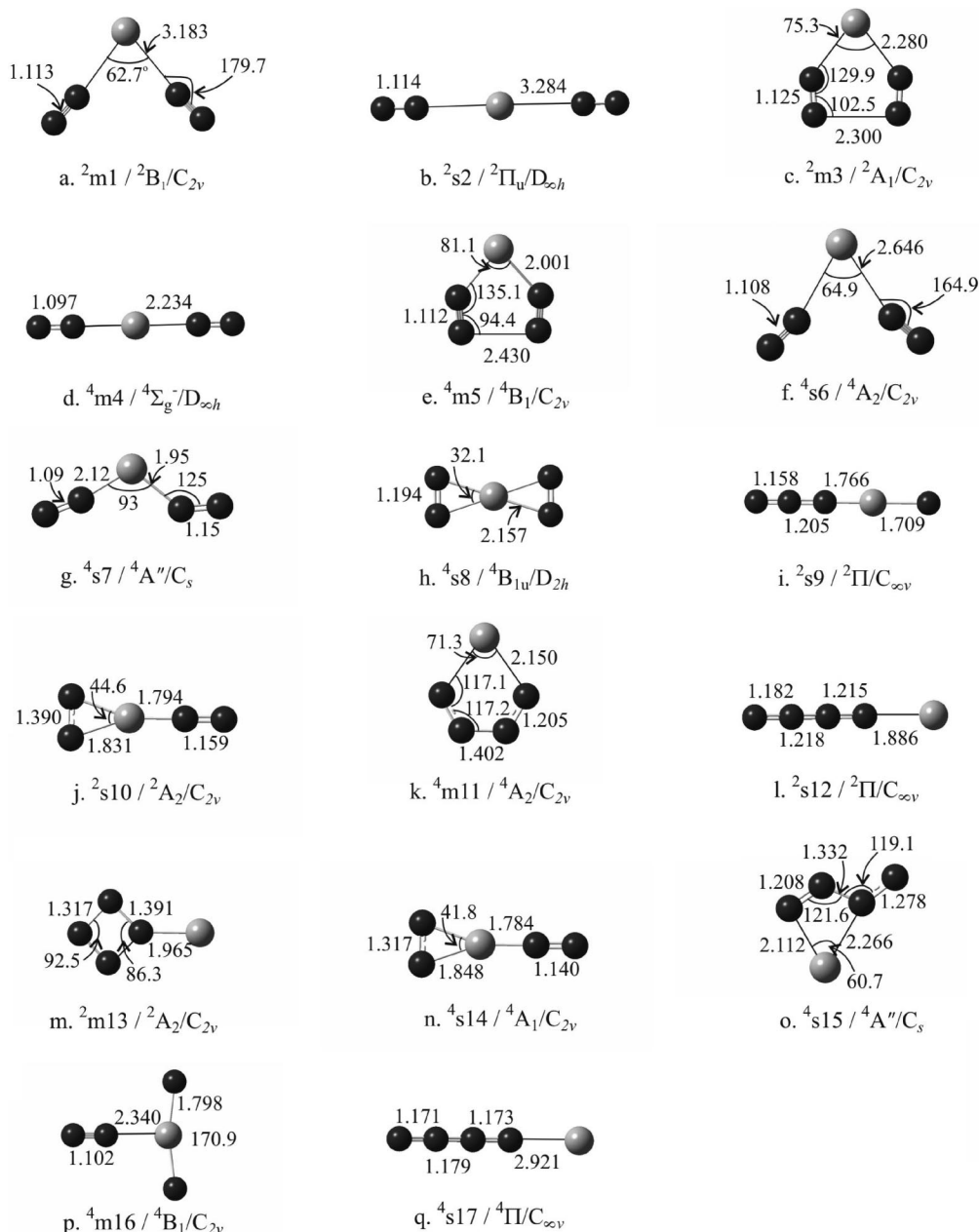


Figure 1. Optimized geometries of 17 structures of doublet and quartet GaN₄ species at MP2/aug-cc-pVTZ level of theory, gray spheres = Ga, black spheres = N.

of -12.9 kcal/mol), but it is bound with respect to Ga(⁴P) + N₂($a^3\Sigma_u^+$) with a D_{e2} of 154 kcal/mol.

The frequency of the N≡N stretching mode is 2186.2 cm⁻¹ in the free N₂($X^1\Sigma_g^+$) molecule at MP2/atz level. In the $\tilde{X}^2\Pi$ and I^2B_2 structures of GaN₂, the corresponding frequencies are blue-shifted by 100 and red-shifted by 12 cm⁻¹, respectively; see Table 2. Moreover, the $\tilde{a}^4\Sigma^-$ structure exhibits a large blue shift of 1016 in this frequency, because the Ga–N bond is short and not a vdW bond, so the N₂ moiety in GaN₂ is more rigid and cannot stretch freely. For the same reason the N–N stretching frequency of the I^4A_2 structure shows a large blue shift of 672 cm⁻¹. Similarly, the I^4B_1 minimum which consists of Ga(⁴P) + N₂($a^3\Sigma_u^+$), presents a very large blue shift of 2052 cm⁻¹ in the N₂ stretching frequency, compared to the corresponding frequency of 1455.2 cm⁻¹ of free N₂($a^3\Sigma_u^+$).

The last two minima listed in Table 1, $I^2\Pi_g$ and $I^4\Pi_u$, correspond to linear symmetric structures, N–Ga–N, with bond

distances $r_{\text{Ga–N}} = 1.767$ and 1.796 Å at MP2_{BSSSE}/atz level, respectively. In both structures, the Ga atom is excited in the ⁴P state.

IV. GaN₄

In the present work, we have calculated 37 structures, 16 minima, and 21 transition states or saddle points of the GaN₄ molecule. The results for the twenty highest-energy structures are given as Supporting Information. The geometries of the remaining 17 structures (7 minima and 10 transition states or saddle points) at the MP2/aug-cc-pVTZ level of theory are summarized in Figure 1. For convenience the structures have been labeled by three symbols the first (superscript) indicates the spin multiplicity (2 or 4), the second the kind of structure, i.e., whether it is a minimum (m) or a saddle point (s) and the third the energy rank of the structure, for instance ²m3 means 2 = doublet, m = minimum and 3 = third lowest energy

TABLE 3: Absolute Energies E_e (hartree), Dissociation Energies and BSSE-corrected Values D_e (BSSE) (kcal/mol), and Geometries $r_{\text{Ga-N}}$, $r_{\text{N-N}}$ (Å), φ_{NGaN} , φ_{GaNN} (degrees) at Different Levels of Theory for the Ground State of GaN_4 , ${}^2\text{m1}(\tilde{X}^2\text{B}_1)$, and ${}^2\text{s2}({}^2\Pi_u)$ Structures

Method	$-E_e$	D_{e1} (BSSE) GaN ₄ → Ga + 4N	D_{e2} (BSSE) GaN ₄ → Ga + 2N ₂	D_{e3} (BSSE) GaN ₄ → GaN ₂ + N ₂	$r_{\text{Ga-N}}$	$r_{\text{N-N}}$	φ_{NGaN}	φ_{GaNN}
${}^2\text{m1}(\tilde{X}^2\text{B}_1)$								
B3LYP/LANL2DZ	221.000832	380.0(377.4)	17.49(10.17)	5.81(1.83)	2.194	1.152	75.0	165.0
B3LYP/DGDZVP	2143.513989	441.3(439.9)	6.08(2.51)	3.02(1.12)	2.572	1.116	71.3	170.3
B3LYP/cc-pVDZ	2143.907398	451.7(446.6)	6.03(2.19)	3.03(1.01)	2.575	1.111	71.8	168.5
B3LYP/SDD	221.027985	377.2(374.5)	14.67(7.80)	5.50(1.82)	2.321	1.150	73.2	168.5
B3PW91/DGDZVP	2143.371876	434.4(432.9)	4.57(1.30)	2.31(0.56)	2.536	1.114	71.7	168.5
PBEPBE/DGDZVP	2142.951939	480.6(478.6)	14.35(9.75)	6.33(3.88)	2.366	1.134	72.9	164.9
LSDA/DGDZVP	2139.939591	555.9(553.6)	31.47(25.79)	14.63(11.57)	2.163	1.132	73.8	160.3
B3LYP/6-311	2143.828287	397.0(389.5)	13.63(5.71)	4.90(0.92)	2.299	1.132	74.1	168.8
B3LYP/6-311+	2143.836189	390.3(383.5)	7.20(0.44)	4.34(1.18)	2.311	1.132	74.0	167.8
B3LYP/6-311G(2df)	2143.953811	463.3(459.8)	4.23(1.84)	2.17(0.94)	2.685	1.096	71.4	170.0
B3LYP/6-311+G(2df)	2143.958472	460.7(459.0)	2.60(1.84)	1.30(0.93)	2.767	1.096	71.5	173.5
B3LYP/6-311+G(3df)	2143.963503	461.7(459.5)	2.49(1.93)	1.25(0.98)	2.793	1.096	71.6	173.7
B3LYP/aug-cc-pVTZ	2144.042288	460.1(459.3)	3.91(3.44)	1.98(1.79)	2.737	1.096	72.0	171.2
MP2/6-311+G(2df)	2141.921128	462.7(455.7)	3.01(1.91)	1.70(1.04)	3.288	1.113	60.8	176.0
MP2/cc-pVTZ	2142.085853	461.1(455.9)	3.56(2.03)	1.96(1.11)	3.186	1.113	62.4	175.3
MP2/aug-cc-pVTZ	2142.104298	466.1(459.6)	4.86(2.43)	2.76(1.39)	3.183	1.113	62.7	179.7
MP4/aug-cc-pVTZ	2142.168235	450.7(445.0)	4.60(2.28)	2.59(1.27)				
${}^2\text{s2}({}^2\Pi_u)$								
B3LYP/LANL2DZ	220.986049	370.8(368.4)	8.21(3.52)	3.47(0.91)	2.734	1.140	180.0	180.0
MP2/6-311+G(2df)	2141.920484	462.3(455.3)	2.60(1.52)	1.29(0.80)	3.359	1.113	180.0	180.0
MP2/cc-pVTZ	2142.085142	460.6(455.6)	3.12(1.74)	1.51(0.83)	3.285	1.113	180.0	180.0
MP2/aug-cc-pVTZ	2142.102550	465.0(459.1)	3.76(2.01)	1.66(1.00)	3.284	1.114	180.0	180.0
MP4/aug-cc-pVTZ	2142.166705	449.9(444.8)	3.64(1.94)	1.63(0.97)				

TABLE 4: GaN_4 Structures Absolute Energies E_e (hartree), Dissociation Energies and BSSE-corrected Values D_e (BSSE) (kcal/mol), Dipole Moments μ (Debye), and Energy Differences ΔE (kcal/mol) at MP2[MP4]/aug-cc-pVTZ Level of Theory

struct	$-E_e$	D_{e1} (BSSE) ^a GaN ₄ → Ga + 4N	D_{e2} (BSSE) ^b GaN ₄ → Ga + 2N ₂	D_{e3} (BSSE) ^c GaN ₄ → GaN ₂ + N ₂	D_{e4} (BSSE) ^d GaN ₄ → Ga + N ₄	μ	ΔE
${}^2\text{m1}$	2142.104298	466.1(459.6)	4.86(2.43)	2.76(1.39)		0.57	0.0
	[2142.168235]	[450.7(445.0)]	[4.60(2.28)]	[2.59(1.27)]			[0.0]
${}^2\text{s2}$	2142.102550	465.0(459.1)	3.76(2.01)	1.66(1.00)		0.0	1.1
	[2142.166705]	[449.9(444.8)]	[3.64(1.94)]	[1.63(0.97)]			[1.0]
${}^2\text{m3}$	2142.073086	446.5(434.4)			148.3(140.6)	2.91	19.6
${}^4\text{m4}$	2141.991615	485.4(474.8)	24.12(17.58)	4.70(1.91)		0.0	70.7
${}^4\text{m5}$	2141.969174	471.3(457.1)	10.04(-0.45)			2.46	84.8
${}^4\text{s6}$	2141.962972	467.4(459.5)	6.15(2.25)			1.49	88.7
${}^4\text{s7}$	2141.958692	464.7(451.0)	3.47(-6.51)			4.05	91.4
${}^4\text{s8}$	2141.927337	445.0(433.6)				0.0	111.0
${}^2\text{s9}$	2141.916270	348.1(332.9)				3.83	118.0
${}^2\text{s10}$	2141.890270	331.8(315.1)				4.07	134.3
${}^4\text{m11}$	2141.889402	331.2(317.6) ^e			48.6(41.0)	1.61	134.8
${}^2\text{s12}$	2141.880288	325.5(312.2)			62.5(54.8)	3.39	140.6
${}^2\text{m13}$	2141.873578	321.3(309.1)			74.8(67.9)	4.62	144.8
${}^4\text{s14}$	2141.865259	406.1(391.6)				2.57	150.0
${}^4\text{s15}$	2141.864245	315.4(302.3) ^e			53.3(44.9)	3.41	150.6
${}^4\text{m16}$	2141.848101	395.3(382.3)				1.14	160.8
${}^4\text{s17}$	2141.784659	265.5(257.6) ^e			3.33(1.45)	1.16	200.6

^a D_e with respect to $\text{Ga}({}^2\text{P}$ and ${}^4\text{P}) + 4\text{N}({}^4\text{S})$ for the doublet and quartet states, respectively. ^b D_e with respect to $\text{Ga}({}^2\text{P}$ and ${}^4\text{P}) + 2\text{N}_2$ ($X^1\Sigma_g^+$) for the doublet and quartet states, respectively. ^c D_e with respect to $\text{GaN}_2(\tilde{X}^2\Pi$ and $\tilde{a}^4\Sigma^-) + \text{N}_2$ ($X^1\Sigma_g^+$) for the doublet and quartet states, respectively. ^d D_e with respect to $\text{Ga}({}^2\text{P})$ + rectangular cyclic $\text{N}_4({}^3\text{B}_2)$ for ${}^2\text{m3}$, $\text{Ga}({}^2\text{P})$ + trapezoid $\text{N}_4({}^3\text{B}_2)$ for ${}^2\text{m11}$, $\text{Ga}({}^2\text{P})$ + linear $\text{N}_4({}^1\Sigma)$ for ${}^2\text{s12}$, $\text{Ga}({}^2\text{P})$ + rhombic $\text{N}_4({}^3\text{B}_2)$ for ${}^2\text{m13}$, and $\text{Ga}({}^2\text{P}) + \text{N}_4({}^3\Sigma)$ for 4s15 and 4s17 . ^e D_e with respect to $\text{Ga}({}^2\text{P}) + 4\text{N}({}^4\text{S})$. With respect to $\text{Ga}({}^4\text{P}) + 4\text{N}({}^4\text{S})$ is 421.2(408.7) for ${}^4\text{m11}$, 405.4 (393.4) for 4s15 , and 355.5(347.8) kcal/mol for ${}^4\text{s17}$.

structure. The results of a DFT study of the ${}^2\text{m1}$ and ${}^2\text{s2}$ structures are presented in Table 3, while for all 17 structures presented here, total energies (E), dissociation energies D_{e1} with respect to $\text{Ga}({}^2\text{P}$ or ${}^4\text{P}) + 4\text{N}({}^4\text{S})$, D_{e2} with respect to $\text{Ga}({}^2\text{P}$ or ${}^4\text{P}) + 2\text{N}_2(X^1\Sigma_g^+)$, D_{e3} with respect to $\text{GaN}_2(\tilde{X}^2\Pi$ or $\tilde{a}^4\Sigma^-) + \text{N}_2(X^1\Sigma_g^+)$, and D_{e4} with respect to $\text{Ga} + \text{N}_4$ (optimized structures of N_4 molecule) as appropriate in each case (see discussion below) and dipole moments are presented in Table 4. Furthermore, their vibrational frequencies and IR intensities are given in Table 5. Figures 2–6 depict the optimized potential energy

profiles with respect to $\text{Ga} + 2\text{N}_2$ or $\text{GaN}_2 + \text{N}_2$, the optimized potential energy curves, and two-dimensional potential energy surfaces of the lowest doublet and quartet minima.

The ground-state of GaN_4 , $\tilde{X}^2\text{B}_1$, is a triangular structure (Figure 1a, ${}^2\text{m1}$), as was in the case of the GaN_4^+ cation, $\tilde{X}^1\text{A}_1$.¹³ The $\tilde{X}^2\text{B}_1$ structure of GaN_4 may be considered as either having two $\text{N}_2(X^1\Sigma_g^+)$ interacting with $\text{Ga}({}^2\text{P})$ via two van der Waals (vdW) bonds which form an angle $\varphi_{\text{NGaN}} = 62.7^\circ$ (MP2/atz level of theory) or having one $\text{GaN}_2(\tilde{X}^2\Pi)$ interacting with a $\text{N}_2(X^1\Sigma_g^+)$. The bond lengths $r_{\text{N-N}}$ and $r_{\text{Ga-N}}$ are similar to the

TABLE 5: Harmonic Frequencies (cm⁻¹) and IR Intensities (km/mol) of the Seven Doublet and Eight Quartet Structures of the GaN₄ Molecule at MP2/cc-pVTZ and MP2/aug-cc-pVTZ Level of Theory

ω	² m1				² s2				² m3		⁴ m4	
	cc-pVTZ		aug-cc-pVTZ		cc-pVTZ		aug-cc-pVTZ		aug-cc-pVTZ		aug-cc-pVTZ	
	ω_e	IR	ω_e	IR	ω_e	IR	ω_e	IR	ω_e	IR	ω_e	IR
ω_1	20.1	0.02	25.5	0.04	5.8	0.04	14.6i	0.06	203.3	14.0	49.5	0.20
ω_2	31.4	0.15	38.6	0.19	13.6	0.01	10.1	0.02	204.9	28.4	49.5	0.20
ω_3	46.1	0	45.9	~0	34.9	0	38.3	0.20	269.6	4.4	84.2	0.25
ω_4	49.1	0.17	49.1	0.14	35.7	0.24	39.9	0.0001	272.0	0.04	187.0	0
ω_5	54.5	0.18	54.9	0.12	39.2	0	44.3	0	373.3	0.04	224.5	0
ω_6	59.9	0.91	57.8	0.86	48.1	0	44.9	0	447.1	2.7	224.5	0
ω_7	73.5	0	86.0	0.04	57.3	1.5	51.6	1.2	1456	970086	298.6	0.88
ω_8	2292	4.2	2330	12.4	80.1	0.44	80.4	0.41	2876	4270	298.6	0.88
ω_9	2293	1.3	2331	3.8	2252	0	2249	0.002	3891	6347	3457	0
ω_{10}					2252	1.9	2249	2.8			3583	1175
ω	⁴ m5		⁴ s6		⁴ s8		² s9		² s10			
	aug-cc-pVTZ		aug-cc-pVTZ		aug-cc-pVTZ		cc-pVTZ		aug-cc-pVTZ		cc-pVTZ	
	ω_e	IR	ω_e	IR	ω_e	IR	ω_e	IR	ω_e	IR	ω_e	IR
ω_1	200.9	0.07	212.2i	0.04	282.1i	0	142.9i	1.9	154.6i	5.0	29.4i	18.7
ω_2	305.3	0.49	62.6	0.78	144.5i	1.83	111.7i	0	115.5i	0.09	101.9	28.4
ω_3	314.6	14.6	76.6	4.6	110.5	1353	142.3	60.2	124.1	60.1	303.9	3.6
ω_4	352.1	151	109.5	0.60	351.7	0	487.0	13.6	480.8	13.8	313.1	3.3
ω_5	356.8	0	125.5	0	364.0	141	532.0	166	514.2	206	521.5	1.9
ω_6	471.3	212	141.8	0.07	419.1	0	568.1	5.3	554.8	3.3	602.2	2.2
ω_7	521.9	18.4	243.9	2.01	461.7	38.7	810.9	5614	747.9	4219	749.2	359
ω_8	3140	330	2980	349	1606	716	1132	2853	1121	2794	1144	476
ω_9	5032	203480	3025	395	1723	0	1574	451	1572	400	2076	35.0
ω_{10}							2472	288	2453	173		
ω	² s10		⁴ m11		² s12		² m13		⁴ s14			
	aug-cc-pVTZ		aug-cc-pVTZ		cc-pVTZ		aug-cc-pVTZ		aug-cc-pVTZ			
	ω_e	IR	ω_e	IR	ω_e	IR	ω_e	IR	ω_e	IR		
ω_1	19.9i	21.9	174.2	4.2	868.5i	4.5	846.8i	4.4	70.1	0.34	440.0i	7.0
ω_2	93.4	31.0	205.2	7.1	477.8i	5.6	437.3i	8.5	74.2	3.3	149.1i	2.4
ω_3	296.4	4.8	334.7	61.5	302.5i	10.1	288.8i	13.0	306.3	71.9	131.1	26.3
ω_4	306.3	3.4	421.6	37.6	8.32i	1.07	56.3	1.7	402.4	14.1	230.2	6.2
ω_5	521.1	2.8	536.9	0	57.4i	1.08	79.3	1.6	416.0	1.33	523.2	4.4
ω_6	606.9	2.7	703.8	620	355.6	96.5	345.1	108	744.0	0.02	568.9	1.7
ω_7	802.1	395	771.5	26.7	461.5	12.7	463.0	12.0	992.7	518	659.2	7.4
ω_8	1144	545	1561	382	1221	873	1216	971	1221	40032	1294	196
ω_9	2062	6.02	2656	20149	1826	5.0	1802	0.81	1431	23.3	2707	80.6
ω_{10}					3810	6263	3804	6207				
ω	⁴ s15		⁴ m16									
	aug-cc-pVTZ		aug-cc-pVTZ									
	ω_e	IR	ω_e	IR								
ω_1	68.71i	2.8	50.5	1.8								
ω_2	172.9	30.2	119.0	6.0								
ω_3	293.5	25.0	153.7	37.9								
ω_4	319.5	0.84	169.1	46.2								
ω_5	358.6	34.0	200.6	21.2								
ω_6	665.8	16.3	300.0	169								
ω_7	1086	44.3	525.0	1470								
ω_8	1129	79.2	684.4	0.002								
ω_9	1556	133	3209	438								

corresponding values in GaN₂ ($\tilde{X}^2\Pi$) at all levels of theory (cf. Tables 1 and 3). It is expected that in this case, as well as in all structures of GaN₄ calculated here, the bond lengths are slightly underestimated since it is not practical to carry out optimizations with respect to the BSSE-corrected energy. As shown in Table 1, this omission leads to an underestimation of the Ga–N bond length in the ground-state of GaN₂ by 0.1 Å.

It might be noted that the cation has a shorter $r_{\text{Ga-N}}$ bond length by ~ 0.5 Å, a larger angle by 9° , and a larger D_{e3} with respect to GaN₂⁽⁺⁾ + N₂ by 3.5 kcal/mol than the neutral

molecule.¹³ Natural population analysis shows practically no charge transfer in the molecule. The spin contamination of the UMP2 calculation is very small with $\langle S^2 \rangle = 0.755$ instead of 0.75.

The results of DFT calculations on ²m1 and on the corresponding linear ²s2 structure are presented in Table 3, i.e., total energies (E), dissociation energies D_{e1} with respect to Ga(²P) + 4N(⁴S), D_{e2} with respect to Ga(²P) + 2N₂($X^1\Sigma_g^+$), and D_{e3} with respect to GaN₂($\tilde{X}^2\Pi$) + N₂($X^1\Sigma_g^+$) and geometries. A series of four functionals, i.e., B3LYP, B3PW91, PBEPBE and

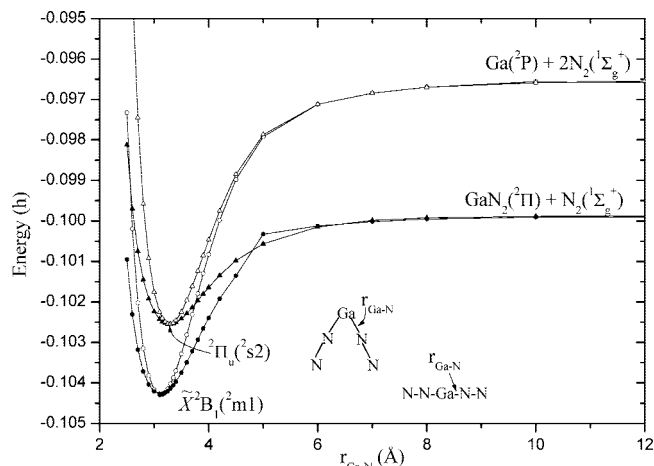


Figure 2. Potential energy curves of the ${}^2m1(\tilde{X}^2B_1)$ and ${}^2s2({}^2\Pi_u)$ isomers of the GaN_4 molecule with respect to the $r_{\text{Ga-N}}$ distance at the MP2/aug-cc-pVTZ level of theory. All energies shifted by +2142.0 h.

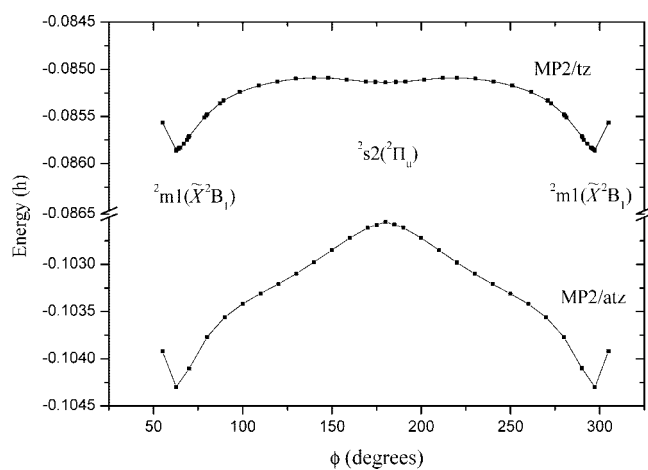


Figure 3. Optimized potential energy profiles ${}^2m1(\tilde{X}^2B_1)$ – ${}^2s2({}^2\Pi_u)$ – ${}^2m1(\tilde{X}^2B_1)$ of the GaN_4 molecule with respect to the ϕ angle. All energies shifted by +2142.0 h.

LSDA and ten basis sets, namely, LANL2DZ, DGDZVP, cc-pVDZ, SDD, 6-311, 6-311+, 6-311G(2df), 6-311+G(2df), 6-311+G(3df), and aug-cc-pVTZ have been employed in different combinations. Additional MP2 and MP4 results were carried out using the 6-311+G(2df), cc-pVTZ, and aug-cc-pVTZ basis sets for reasons of comparison. As shown in Table 3, the DFT results deviate significantly from the corresponding MP2 and MP4. For the geometry, our best result is $r_{\text{Ga-N}} = 3.183$ Å (MP2/atz) while the DFT methods give $r_{\text{Ga-N}}$ values ranging from 2.163 to 2.793 Å, showing a reduction of up to 32%. The BSSE corrected dissociation energy with respect to $\text{Ga} + 2\text{N}_2$ is $D_{e2} = 2.4(2.3)$ kcal/mol and with respect to $\text{GaN}_2 + \text{N}_2$ is $D_{e3} = 1.4(1.3)$ kcal/mol at MP2/atz(MP4/atz//MP2/atz) level of theory. The corresponding DFT values are $D_{e2} = 0.44 - 25.8$ kcal/mol and $D_{e3} = 0.56 - 11.6$ kcal/mol. All the above show that the DFT methodology does not predict correctly the geometry and especially the dissociation energy of the global minimum, ${}^2m1(\tilde{X}^2B_1)$, of the vdW GaN_4 molecule compared to the MP2 and MP4 methods. It is obvious that the weakness of the DFT to predict the dispersion energy for weak vdW systems³² results in yielding insufficiently accurate results. It seems that B3LYP is the most appropriate functional, but even with that, in conjunction with a large basis set of augmented triple- ζ quality, the results of the DFT calculations are not

sufficiently good; see Table 3. This is of course not unexpected, as the shortcomings of the DFT method for weakly bound systems are well known.

As far as we know, there is only one previous study for the GaN_4 molecule, that of Song et al.,¹² who calculated three isomers using the full potential linear muffin tin orbital method, and their lowest isomer, which is the same structure as ours, has 36% shorter bond distance Ga–N than ours, showing again that such methods are not adequate for van der Waals systems.

The MP2/atz potential energy profiles of the ${}^2m1(\tilde{X}^2B_1)$ and ${}^2s2({}^2\Pi_u)$ structures of the GaN_4 molecule are plotted in Figure 2 as one or two N_2 molecules are being removed. The optimized potential energy profile of the ground state, ${}^2m1(\tilde{X}^2B_1)$ with respect to the angle ϕ (i.e., the bending potential) at MP2/tz (upper curve) and MP2/atz levels are shown in Figure 3. Along this profile, structure ${}^2s2({}^2\Pi_u)$ is a transition state at the MP2/atz level, but has no imaginary frequencies at the MP2/tz level. It should be noted that the corresponding BSSE optimized potential energy profiles at MP2/tz and MP2/atz level have exactly the same shapes as those in Figure 3, which means that diffuse functions are necessary to determine what type of extremum ${}^2s2({}^2\Pi_u)$ is. In the case of the GaN_4^+ cation¹³ the corresponding linear $\text{N}\equiv\text{N}\cdots\text{Ga}^+\cdots\text{N}\equiv\text{N}$ isomer is a transition state in both MP2/tz and MP2/atz level of theory.

Isomerization between two equivalent \tilde{X}^2B_1 minima, as the wedge changes direction, occurs via the transition state, the linear 2s2 , (Figure 1b), which has an increased $r_{\text{Ga-N}}$ bond by ~ 0.1 Å at the MP2/atz level of theory while the barrier to isomerization is 1.1 kcal/mol; see Table 4. A contour plot of the optimized two-dimensional potential energy surface between the two ${}^2m1(\tilde{X}^2B_1)$ minima and their transition state ${}^2s2({}^2\Pi_u)$ at the MP2/atz level is given in Figure 4.

Harmonic frequencies of 2m1 and 2s2 at MP2/tz and MP2/atz level of theory are given in Table 5. The frequencies ω_2 to ω_7 (2m1) and ω_3 to ω_8 (2s2) are all within a narrow range of 10 cm^{-1} ; consequently the ordering of frequencies of stretching and bending modes is different in the two basis sets. Compared to the frequencies of the modes of $\text{GaN}_2(\tilde{X}^2\Pi)$ and $\text{GaN}_4({}^2m1)$, they show small shifts ranging in an interval of ± 44 cm^{-1} . The one imaginary frequency of 2s2 corresponds to the bending of the linear N-N-Ga-N-N .

The third isomer 2m3 is a cyclic minimum (see Figure 1c) with $r_{\text{Ga-N}} = 2.280$ Å and $\varphi_{\text{NGaN}} = 75.3^\circ$ at the MP2/atz level of theory. Natural population analysis shows that the net charge of the Ga is $+0.69$ e^{-1} while the adjacent N atoms to Ga atom are negative with a net charge of -0.29 e^{-1} . This structure is unbound with respect to $\text{Ga}({}^2P) + 2\text{N}_2(X^1\Sigma_g^+)$. However, from the geometry of the molecule, it seems that Ga (2P) interacts with a rectangular cyclic $\text{N}_4({}^3B_2)$ and the BSSE corrected dissociation energy with respect to $\text{Ga}({}^2P) + \text{N}_4({}^3B_2)$ (optimized local minimum of the N_4 molecule) is 140.6 kcal/mol.

The 4m4 , 4m5 , 4s6 , and 4s7 structures consist of a Ga atom in its excited state 4P interacting with two $\text{N}_2(X^1\Sigma_g^+)$ molecules; see Figure 1d–g. Of these structures, the lowest-energy one, ${}^4m4({}^4\Sigma_g^-)$, which is the third minimum calculated for GaN_4 , is a linear structure lying 70.7 kcal/mol above the 2m1 minimum, while the remaining three structures are bent with different values for the φ_{NNGa} angle. The BSSE corrected dissociation energy with respect to $\text{Ga}({}^4P) + 2\text{N}_2(X^1\Sigma_g^+)$ is 17.6 kcal/mol and with respect to $\text{GaN}_2(\tilde{a}^4\Sigma^-) + \text{N}_2(X^1\Sigma_g^+)$ is 1.9 kcal/mol for the 4m4 isomer. The 4m5 minimum is a cyclic minimum and it lies 14.1 kcal/mol above the linear 4m4 isomer. It should be noted that some DFT calculations give larger φ_{NNGa} and φ_{NGaN} angles than the MP2 leading to an open cyclic minimum

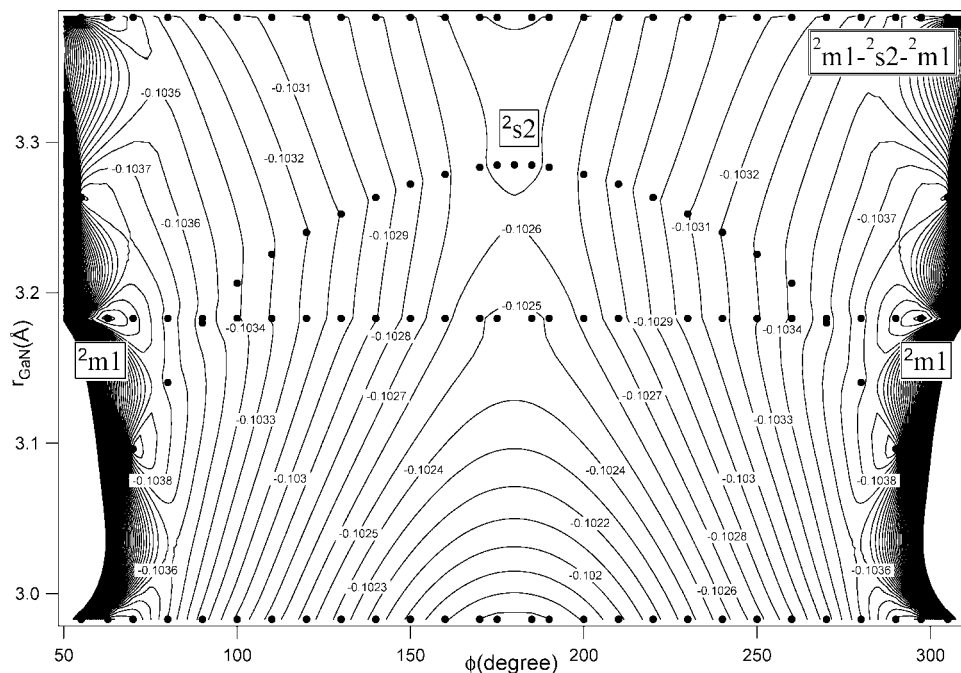


Figure 4. Potential energy surface of ${}^2m1(\bar{X}^2B_1) \rightarrow {}^2s2(2\Pi_u) \rightarrow {}^2m1(\bar{X}^2B_1)$ as a function of the Ga–N distance and the ϕ_{NGaN} angle represented by contour lines equally spaced by 0.0001 hartree at the MP2/aug-cc-pVTZ level of theory. The contour lines were drawn based on the data calculated at the coordinates represented by the filled circles.

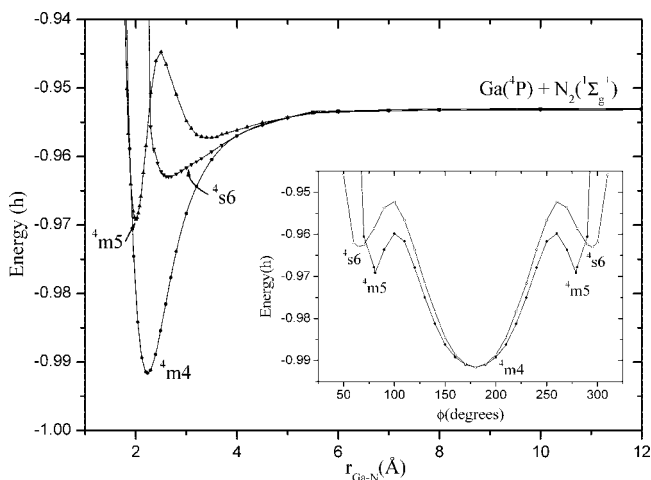


Figure 5. Potential energy curves of the ${}^2m4({}^4\Sigma_g^-)$, ${}^4m5({}^4B_1)$, and ${}^4s6({}^4A_2)$ states of the GaN₄ molecule with respect to the $r_{\text{Ga-N}}$ distance at the MP2/aug-cc-pVTZ level of theory. Inset: optimized potential energy profiles of the GaN₄ ${}^2m4({}^4\Sigma_g^-) \rightarrow {}^4m5({}^4B_1)$ and ${}^2m4({}^4\Sigma_g^-) \rightarrow {}^4s6({}^4A_2)$ with respect to the ϕ angle. All energies shifted by +2141.0 h.

(see Supporting Information). Comparing the lowest quartet and doublet states of GaN₄, we observe that the quartet global minimum is linear, while the doublet global minimum is bent. Moreover, the dissociation energy of 4m4 is larger than that of 2m1 , 17.6 versus 2.4 kcal/mol with respect to the adiabatic products Ga + 2N₂, respectively. It might be noted that in the case of the GaN₄⁺ cation¹³ the lowest minimum is a spin singlet and has bent structure as in the case of GaN₄, while the lowest triplet minimum of GaN₄⁺, which has the Ga⁺ cation excited, is also a bent structure with a BSSE dissociation energy of 43.5 kcal/mol with respect to Ga⁺(³P) + 2N₂ while the linear structure is a transition state contrary to the linear quartet global minimum of GaN₄. Finally, we should report that the spin contamination of UMP2 calculation of the quartet 4m4 is very small, with $\langle S^2 \rangle = 3.751$ instead of 3.75.

The potential energy curves of 4m4 , 4m5 , and 4s6 with respect to dissociation to the limit Ga(⁴P) + N₂(¹ Σ_g^+) are plotted in Figure 5. The potential energy curve for 4m5 shows the existence of a barrier with respect to this motion. The barrier persists with different computational approaches and it would seem that it could be the result of an avoided crossing with an excited state, which however has ground-state N₂, since the N₂ moiety appears to be in the same state throughout the potential energy curve.

The optimized potential energy profiles of ${}^4m5 \rightarrow {}^4m4 \rightarrow {}^4m5$ and of ${}^4s6 \rightarrow {}^4m4 \rightarrow {}^4s6$ with respect to the bending angle are depicted in the insets of Figure 5. The 4m5 and 4s6 isomers have to overcome a barrier of 5.9 and 6.7 kcal/mol, respectively, to reach the 4m4 minimum. A two-dimensional picture is given by the contour plot of the potential energy surface (see Figure 6) showing one 4m4 , two 4m5 , and two 4s6 structures.

The frequencies of vibrational modes of 4m4 and 4m5 are given in Table 5. Comparing these values to those of GaN₂($\bar{a}^4\Sigma^-$) and N₂, we observe the largest differences in the last two ω frequencies, corresponding to stretching of the two N≡N. The ω_9 (4m4) presents a large blue shift of 1271 with respect to the free N₂ similar to the 1016 cm⁻¹ shift in GaN₂($\bar{a}^4\Sigma^-$), while ω_{10} (4m4), which corresponds to “asymmetric stretch” (one N–N increasing and the other N–N decreasing), shows an even larger shift of 1397 cm⁻¹ with respect to the symmetric stretch of free N₂. These large blue shifts result from the fact that the N₂ in GaN₄(4m4) are rigid and cannot stretch freely. In 4m5 , the ω_8 and ω_9 values are blue-shifted by 954 and 2846 cm⁻¹ compared to the ω of the free N₂ molecule, which is consistent with the fact that the 4m5 minimum is bent and the two N₂ molecules are closer to each other.

In 4m4 , the natural population analysis shows only a small charge transfer, the Ga atom possessing a net charge of $-0.05e^-$, the N atoms at the end have a positive charge of about $+0.07$ each, while the N atom closer to Ga has gained -0.04 e^- . In 4m5 , larger charge transfers are observed, the Ga atom is positively charged with a net charge of $+0.63$ e^- , the

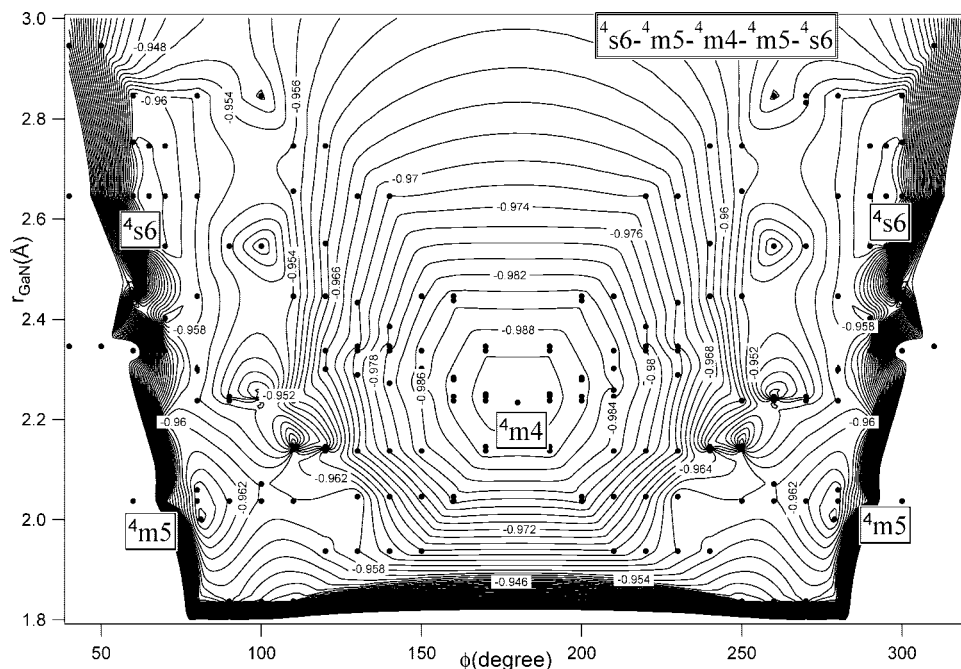


Figure 6. Potential energy surface of ${}^4s6-{}^4m5-{}^4m4-{}^4m5-{}^4s6$ as a function of the Ga–N distance and the φ_{NGaN} angle represented by contour lines equally spaced by 0.002 hartree at the MP2/aug-cc-pVTZ level of theory. The contour lines were drawn based on the data calculated at the coordinates represented by the filled circles.

N atoms at the end have about -0.02 each, while the N atom closer to Ga has gained -0.29 e^- .

The 4m11 isomer is a cyclic minimum with quartet spin symmetry, see Figure 1k, with $r_{\text{Ga-N}} = 2.150$ Å and $\varphi_{\text{NGaN}} = 71.3^\circ$ at the MP2/atz level of theory. Natural population analysis shows that the Ga atom is in its ground state, 2P , with a net charge of $+0.71$ e^- while the adjacent N atoms are negative with a net charge of -0.35 e^- . Thus, the Ga(2P) atom is connected to a trapezoid ${}^3N_4({}^3B_2)$ molecule. The BSSE corrected dissociation energy with respect to Ga(2P) + optimized ${}^3N_4({}^3B_2)$ is 41.0 kcal/mol.

The ${}^4s8({}^4B_{1u})$ is a saddle point of D_{2h} symmetry (see Figure 1h), and the imaginary frequencies correspond to movements of N_2 out of the plane of the molecule. It consists of Ga(2P) + 2 $N_2({}^3\Pi_g)$ with a BSSE diabatic binding energy of 232 kcal/mol. The 2s10 and 4s14 isomers are T-shaped structures consisting of either a triangular GaN $_2$ and a N_2 connected with a bond to Ga, or a linear GaNN whose Ga interacts with the N_2 triple bond; see Figure 1j,n. The 2s10 isomer has one frequency which corresponds to a movement in the plane of the N_2 around the C_2 axes and the 4s14 isomer has two imaginary frequencies which correspond the first one to a movement of the N_2 molecules out of plane and the second one in the plane. Both isomers have an excited Ga(4P) and a triplet excited N_2 whose triple bond interacts with the Ga atom. The BSSE corrected dissociation energies of the isomers with respect to $N_2(X^1\Sigma_g^+) + N_2({}^3\Sigma_u^+) + Ga({}^4P)$ are 114(2s10) and 98(4s14) kcal/mol, while they are unbound with respect to the ground-state products Ga(2P) + 2 $N_2(X^1\Sigma_g^+)$.

The 2s9 , 2s12 , and 4s17 isomers are linear structures; see Figure 1, panels i, l, and q, respectively. All structures have the Ga atom in the ground state 2P . The BSSE corrected dissociation energy with respect to Ga(2P) + optimized $N_4({}^1\Sigma)$ is 54.8 kcal/mol for 2s12 and with respect to Ga(2P) + optimized $N_4({}^3\Sigma)$ is 1.5 kcal/mol for 4s17 .

The 2m13 isomer consists of a cyclic N_4 molecule connected to the Ga(2P) atom. The BSSE corrected dissociation energy

with respect to Ga(2P) + optimized cyclic $N_4({}^3B_2)$ is 67.9 kcal/mol. The 4s15 isomer has one imaginary frequency which corresponds to a movement of N_4 out of plane. It consists of Ga(2P) interacting with a triplet N_4 with a BSSE corrected dissociation energy of 44.9 kcal/mol. Finally, the 4m16 minimum consists of Ga(4P) connected with two N atoms and one $N_2(X^1\Sigma_g^+)$, see Figure 1p. The BSSE corrected dissociation energy with respect to Ga(4P) + 2N(4S) + $N_2(X^1\Sigma_g^+)$ is 153.7 kcal/mol.

V. Conclusions and Comments

Employing perturbation theory (MP2, MP4/aug-cc-pVTZ) the gallium dinitride, GaN $_2$ and the gallium tetranitride molecules, GaN $_4$, were systematically examined. Seven (GaN $_2$) and thirty-seven (GaN $_4$) electronic structures were determined. Their geometries, dissociation energies, and harmonic frequencies are reported, and potential energy profiles, potential energy surfaces, and the bonding mechanisms of some lowest states are given. Our findings can be summarized as follows.

1. The ground-state of GaN $_2$ ($\tilde{X}^2\Pi$) is a linear van der Waals molecule $N\equiv N\cdots Ga$ with $r_{\text{Ga-N}} = 3.306$ Å and dissociation energy of 1.1 kcal/mol with respect to Ga(2P) + $N_2(X^1\Sigma_g^+)$ products.

2. The next minimum is the $\tilde{a}^4\Sigma^-$ state ($NNGa^+$, $r_{\text{Ga-N}} = 2.002$ Å) and the reaction energy of GaN $_2(\tilde{a}^4\Sigma^-) \rightarrow Ga({}^2P) + N_2(X^1\Sigma_g^+)$ is 14.5 kcal/mol.

3. The ground electronic state of GaN $_4$ is a triangular structure of ${}^2B_1(C_{2v})$ symmetry with a D_e of 2.4 and 1.4 kcal/mol with respect to Ga(2P) + 2 $N_2(X^1\Sigma_g^+)$ and to GaN $_2(\tilde{X}^2\Pi) + N_2(X^1\Sigma_g^+)$, respectively. The energy of isomerization between two equivalent \tilde{X}^2B_1 as the wedge changes direction via a linear state (N–N–Ga–N–N) is 1.1 kcal/mol.

4. The second (2A_1) minimum is a cyclic structure, lying 19.6 kcal/mol above the ground state.

5. The lowest quartet minimum of GaN $_4$ is a linear structure of ${}^4\Sigma_g^- (D_{\infty h})$ symmetry with a $D_e = 17.6$ and 1.9 kcal/mol

with respect to Ga(⁴P) + 2N₂(X¹Σ_g⁺) and GaN₂($\tilde{a}^4\Sigma^-$) + N₂(X¹Σ_g⁺), respectively.

6. A DFT study of the ground-state of GaN₄, employing different combinations of functionals and basis sets did not yield sufficiently accurate results, as might be expected since GaN₄ is a weakly bound and the dispersion energy of such systems usually is not well described by DFT. It seems that of the different combinations examined, B3LYP in conjunction with a large basis set of augmented triple- ζ quality gives the best results within the DFT methodology.

Acknowledgment. Financial support has been provided by the Greek General Secretariat for Research and Technology through a Greece-Slovakia bilateral collaboration program. Partial support of this work through the "Excellence in the Research Institutes" program, supervised by the General Secretariat for Research and Technology/Ministry of Development, Greece (Phase I and II, Projects 64769 and 2005ΣΕ01330081), is gratefully acknowledged.

Supporting Information Available: The optimized geometries of all 37 structures of doublet and quartet GaN₄ species at DFT(B3LYP/LANL2DZ) and MP2/[6-311+G(2df), cc-pVTZ, and aug-cc-pVTZ] level of theory are provided. This material is available free of charge via the Internet at <http://pubs.acs.org>.

References and Notes

- (1) Matsubara, H.; Yoshimoto, S.; Saito, H.; Jianglin, Y.; Tanala, Y.; Noda, S. *Science* **2008**, *319*, 445.
- (2) Goldberger, J.; He, R.; Zhang, Y.; Lee, S.; Yan, H.; Choi, H.-J.; Yang, P. *Nature* **2003**, *422*, 599.
- (3) Nakamura, S. *Science* **1998**, *281*, 956.
- (4) For example, Fuchs, M.; Da Silva, J. L. F.; Stampfl, C.; Neugebauer, J.; Scheffler, M. *Phys. Rev. B* **2002**, *65*, 245212.
- (5) BelBruno, J. J. *Heteroat. Chem.* **2000**, *11*, 281.
- (6) Kandalam, A. K.; Blanco, M. A.; Pandey, R. *J. Phys. Chem. B* **2001**, *105*, 6080. 2002, *106*, 1945.
- (7) Denis, P. A.; Balasubramanian, K. *Chem. Phys. Lett.* **2006**, *423*, 247.
- (8) Šimová, L.; Tzeli, D.; Urban, M.; Černušák, I.; Petsalakis, I.; Theodorakopoulos, G. *Chem. Phys.* **2008**, *349*, 98.
- (9) Kandalam, A. K.; Pandey, R.; Blanco, M. A.; Costales, A.; Recio, J. M.; Newsam, J. M. *J. Phys. Chem. B* **2000**, *104*, 4361.
- (10) Zhou, M.; Andrews, L. *J. Phys. Chem. A* **2000**, *104*, 1648.
- (11) Wang, C.-S.; Balasubramanian, K. *Chem. Phys. Lett.* **2004**, *404*, 294.
- (12) Song, B.; Cao, P.-L. *Phys. Lett. A* **2004**, *328*, 364.

- (13) Tzeli, D.; Petsalakis, I.; Theodorakopoulos, G. *J. Phys. Chem. A* **2007**, *111*, 8892.
- (14) Becke, A. D. *J. Chem. Phys.* **1993**, *98*, 1372.
- (15) Lee, C.; Yang, W.; Parr, R. G. *Phys. Rev. B* **1988**, *37*, 785.
- (16) Hay, P. J.; Wadt, W. R. *J. Chem. Phys.* **1985**, *82*, 299.
- (17) (a) Becke, A. D. *J. Chem. Phys.* **1993**, *98*, 5648. (b) Perdew, J. P.; Wang, Y. *Phys. Rev. B* **1992**, *45*, 13244.
- (18) Perdew, J. P.; Burke, K.; Ernzerhov, M. *Phys. Rev. Lett.* **1997**, *78*, 1396.
- (19) (a) Vosko, S. H.; Wilk, L.; Nusair, M. *Canadian J. Phys.* **1980**, *58*, 1200. (b) Hohenberg, P.; Kohn, W. *Phys. Rev. B* **1964**, *136*, 864.
- (20) Godbout, N.; Salahub, D. R.; Andzelm, J.; Wimmer, E. *Can. J. Chem.* **1992**, *70*, 560.
- (21) (a) Dunning, T. H., Jr. *J. Chem. Phys.* **1989**, *90*, 1007. (b) Wilson, A. K.; Wood, D. E.; Peterson, K. A.; Dunning, T. H., Jr. *J. Chem. Phys.* **1999**, *110*, 7667.
- (22) Igel-Mann, G.; Stoll, H.; Preuss, H. *Mol. Phys.* **1988**, *65*, 1321.
- (23) Curtiss, L. A.; McGrath, M. P.; Blandeau, J.-P.; Davis, N. E.; Binning, R. C., Jr.; Radom, L. *J. Chem. Phys.* **1995**, *103*, 6104.
- (24) Demovič, L.; Černušák, I.; Theodorakopoulos, G.; Petsalakis, I. D.; Urban, M. *Chem. Phys. Lett.* **2007**, *447*, 215.
- (25) Tzeli, D.; Tsekouras, A. A. *J. Chem. Phys.* **2008**, *128*, 144103.
- (26) (a) Boys, S. F.; Bernardi, F. *Mol. Phys.* **1970**, *19*, 553. (b) Liu, B.; Mclean, A. D. *J. Chem. Phys.* **1973**, *59*, 4557. (c) Jansen, H. B.; Ros, P. *Chem. Phys. Lett.* **1969**, *3*, 140.
- (27) Tzeli, D.; Mavridis, A.; Xantheas, S. S. *J. Phys. Chem. A* **2002**, *106*, 11327.
- (28) Jeziorski, B.; Moszynski, R.; Szalewicz, K. *Chem. Rev.* **1994**, *94*, 1887.
- (29) Simon, S.; Duran, M.; Dannenberg, J. J. *J. Chem. Phys.* **1996**, *105*, 11024.
- (30) Frisch, M. J.; Trucks, G. W.; Schlegel, H. B.; Scuseria, G. E.; Robb, M. A.; Cheeseman, J. R.; Montgomery, J. A. Jr.; Vreven, T.; Kudin, K. N.; Burant, J. C.; Millam, J. M.; Iyengar, S. S.; Tomasi, J.; Barone, V.; Mennucci, B.; Cossi, M.; Scalmani, G.; Rega, N.; Petersson, G. A.; Nakatsuji, H.; Hada, M.; Ehara, M.; Toyota, K.; Fukuda, R.; Hasegawa, J.; Ishida, M.; Nakajima, T.; Honda, Y.; Kitao, O.; Nakai, H.; Klene, M.; Li, X.; Knox, J. E.; Hratchian, H. P.; Cross, J. B.; Adamo, C.; Jaramillo, J.; Gomperts, R.; Stratmann, R. E.; Yazyev, O.; Austin, A. J.; Cammi, R.; Pomelli, C.; Ochterski, J. W.; Ayala, P. Y.; Morokuma, K.; Voth, G. A.; Salvador, P.; Dannenberg, J. J.; Zakrzewski, V. G.; Dapprich, S.; Daniels, A. D.; Strain, M. C.; Farkas, O.; Malick, D. K.; Rabuck, A. D.; Raghavachari, K.; Foresman, J. B.; Ortiz, J. V.; Cui, Q.; Baboul, A. G.; Clifford, S.; Cioslowski, J.; Stefanov, B. B.; Liu, G.; Liashenko, A.; Piskorz, P.; Komaromi, I.; Martin, R. L.; Fox, D. J.; Keith, T.; Al-Laham, M. A.; Peng, C. Y.; Nanayakkara, A.; Challacombe, M.; Gill, P. M. W.; Johnson, B.; Chen, W.; Wong, M. W.; Gonzalez, C.; Pople, J. A.; *Gaussian 03*, revision C.02; Gaussian, Inc.: Wallingford, CT, 2004.
- (31) Huber, K. P.; Herzberg, G. *Molecular Spectra and Molecular Structure. IV Constants of diatomic molecules*; Van Nostrand Reinhold Company: New York, 1979.
- (32) Koch, W.; Holthausen, M. C. *A Chemist's Guide to Density Functional Theory*; 2nd Edition: Wiley-VCH: Weinheim, 2001.

JP8019396